Journal of Magnetic Resonance 214 (2012) 175–183

Contents lists available at SciVerse ScienceDirect

Journal of Magnetic Resonance

journal homepage: www.elsevier.com/locate/jmr

Rapid spectroscopic velocity quantification using periodically oscillating gradients

Constanze Schelhorn [a], Peter Michael Jakob [a,b], Florian Fidler [a,*]

[a] Research Center Magnetic-Resonance-Bavaria, Am Hubland, D-97074 Würzburg, Germany
[b] Dept. of Experimental Physics, 5, University of Würzburg, Am Hubland, D-97074 Würzburg, Germany

ARTICLE INFO

Article history:
Received 8 November 2010
Revised 27 October 2011
Available online 17 November 2011

Keywords:
Flow quantification
Oscillating gradients
MR spectroscopy

ABSTRACT

In this work two spectroscopic methods are described which allow rapid flow velocity quantification in the presence of a parabolic velocity distribution. This method requires only a single excitation and is based on flow encoding by periodically oscillating gradients. In the shown spin echo variant additional refocusing pulses correct for field inhomogeneities. A theoretical model is introduced, which describes the course of the derived spectra even in high flow region, where a significant part of the encoded spins leaves the sensitive area of the coil during data acquisition (outflow-effect). It was demonstrated that both methods can quantify flow velocities within the velocity range of 1 mm/s up to 36 cm/s in the presence of a parabolic flow velocity distribution. The maximum velocity of the parabolic distribution is indicated in this method by a peak in the acquired spectrum from which the velocity could be quantified. Flow velocity quantification by periodically oscillating gradients seems a reasonable and fast alternative to established imaging techniques.

1. Introduction

Flow and motion sensitivity of nuclear magnetic resonance have been known for a long time [4,10,5]. Several techniques for measuring flow are based on changes in the phase of the signal because of the effect of magnetic-field gradients on moving spins [6]. Common phase-sensitive methods are phase-contrast [8,3] and Fourier velocity encoding [2,1]. These methods have in common that they either give an average velocity over the voxel or in case of imaging over a single pixel. By these techniques velocity images are obtained, which can detect regional variations of motion. In general phase-contrast imaging methods provide information about an average of all covered velocities in the probe. This is due to a single encoding step between excitation and data readout. Flow velocity profiles can be achieved by repetition of flow encoding step with different gradient strength. Typically flow profiles are measured by spatial encoding, as for velocity distributions (e.g. laminar flow) different flow velocities are coupled with different spatial positions [9]. Imaging methods require spatial encoding and therefore depending on the desired resolution a large number of encoding steps resulting in a long acquisition time. Consequently it is difficult to measure rapid changes of motion in time. Apart from imaging techniques, the concept of velocity spectral encoding using periodically oscillating gradients/*alternating current* (*AC*) gradients has been demonstrated [7]. In this work a method is presented which is based on the paper of Walton et al. It was shown that velocity spectra can be measured by applying an oscillating gradient in the flow direction of interest. To acquire a complete spectrum only one excitation is needed. Signal detection is similar to the acquisition of a free induction decay with a low bandwidth. The time between acquisition of data points is used for fast flow encoding. In case of the spin echo variant shown here magnetization is additionally refocused by a pulse between each data point. This technique implies the possibility to quantitatively measure velocities without the need of spatial encoding. The work of Walton et al. showed a proof of principle for spectroscopic flow measurements demonstrating that flow can be detected by the occurrence of a frequency shift in the acquired spectrum. However, only a qualitatively examination of this method regarding the effects of velocity distributions on the course of the spectrum for high flow velocities were performed.

In this paper we provide a theoretical model, describing in particular how parabolic velocity distributions influence the course of the derived spectra. For this purpose simulations of the flow encoded spectra were performed. Additionally a theoretical model considering deviations caused by high flow velocities was developed. It considers deviations from spins leaving the sensitive volume of the receive coil during signal reception.

One gradient-echo-based and one spin-echo-based pulse sequence applying this principle of flow encoding were implemented on a NMR spectrometer. Furthermore experiments with a flow phantom were carried out and the results of the velocity distributions as well as quantitative measurements of velocities are presented. The time for data acquisition is in the order of T_2^* referring to the gradient echo version in the order of T_2 for the spin

* Corresponding author. Fax: +49 (0)931 318 4680.
E-mail address: fidler@mr-bavaria.de (F. Fidler).

1090-7807/$ - see front matter © 2011 Elsevier Inc. All rights reserved.
doi:10.1016/j.jmr.2011.11.005

echo version, respectively. As only one excitation is needed to acquire a complete data set, this a fast technique for measuring velocities.

2. Methods

2.1. Theory

The basic idea of flow-encoding by periodically oscillating gradients is similar to flow encoding in phase-contrast experiments by bipolar gradients. After excitation a periodically oscillating gradient is applied, whose dc-component equals to zero. The magnetization is rephased periodically after every period of the gradient and thus generating an echo. Basically a periodically phase encoding is performed as well as stroboscopic readout after each encoding step, e.g. after each period of the gradient. Similar to phase-contrast methods flowing spins accumulate an additional phase $\phi(t)$ depending on their flow velocity v. Due to the gradient the phase of the stationary spins as well as the flowing spins is effected as following:

$$\phi(t) = \gamma \int_0^t G(t')x(t')dt', \quad (1)$$

where $x(t) = x_0 + vt$ is the position of the particle moving with constant velocity. We assume that G and v are parallel. A simple waveshape for the gradient is sinusoidal. On the basis of a sinusoidal gradient with angular frequency ω_G and a peak amplitude G the effect of the gradient on the flowing spins is explained:

$$\phi(t) = \gamma G \int_0^t sin(\omega_G t')[x_0 + \dot{x}t']dt'. \quad (2)$$

The evaluation of the above integral for $t = \frac{n}{\omega_G}$, where $n \in \mathbb{N}$, e.g. an integer number of cycles of gradients after the excitation, leads to the following equation for the time-dependent phase:

$$\phi(t) = -\frac{\gamma G v}{\omega_G} t \quad (3)$$

This phase accumulation is ergo linear in time (for the stroboscopic values of t, e.g. at the time of readout).

Furthermore the instantaneous precession frequency in the rotating frame $\omega(t)$ is

$$\omega(t) = \frac{\partial \phi}{\partial t}. \quad (4)$$

Using Eqs. (4) and (3) it is obvious that due to the phase shift a frequency shift $\Delta\omega$ occurred.

$$\Delta v = \frac{\Delta\omega}{2\pi} = -\frac{\gamma G}{2\pi} \frac{1}{\omega_G} v \quad (5)$$

Consequently the Fourier transformation of the time-domain signal shows a shift of frequency directly proportional to the velocity of the spins. Assuming a velocity distribution in the sample, this distribution will be represented by a frequency shift distribution in the spectra. Therefore flow-encoding by oscillating gradients offers the possibility to measure a velocity distribution due to the velocity induced shift in the frequency domain.

2.2. Pulse sequence – AC Gradient Echo

One realization of the described principle is the AC Gradient Echo (ACGE) (see Fig. 1a). The magnetization is flipped into the transverse plane by a 90° pulse. The timing of the pulse was chosen to coincide with the zero crossing of the gradient. In general two echoes per cycle of the gradient occur, whenever the time integral of the gradient becomes zero (see Fig. 1b). At these moments the stationary spins have no phase accumulation, therefore have the same frequency in the rotating frame. One echo in each cycle is fixed at an integer number of cycles after the excitation pulse. The location of the second echo can be adjusted by varying the position of the pulse relative to the phase of the gradient. Locating the pulse at the zero crossing of the gradient and ergo all subsequent echoes, the two echoes superimpose, which leads to an echo of maximum intensity (Fig. 1a). The sampling of the data is carried out at the positive-slope zero crossing of the sinusoidal gradient.

2.3. Pulse sequence – AC Spin Echo

A second implementation of flow-encoding by periodically oscillating gradients is the AC Spin Echo (ACSE) sequence. The basic timing scheme is the same used for the ACGE. Additionally a 180° pulse train is implemented at the negative-slope zero crossing of the sine gradient. The characteristic of every 180° pulse to invert the magnetization leads to the concept of *effective gradients*, which differ from the physically applied ones. In the case of a sinusoidal gradient, the effective gradient is depicted in the lower portion of Fig. 2 (dotted line). As a consequence the integral of the effective gradient is equal to zero only at even echoes, thus the odd echoes are not expected to occur. The effective angular frequency of the sine-like gradient is therefore $\omega_{G_{eff}} = \frac{\omega_G}{2}$. To calculate the frequency shift as a function of velocity (see Eq. (5)), ω_G has to be replaced with $\omega_{G_{eff}}$. Compared to the ACGE the resulting frequency shift at constant parameters is twice as large as in the ACSE. The data acquisition is carried out at exactly the same moments as in the gradient echo method.

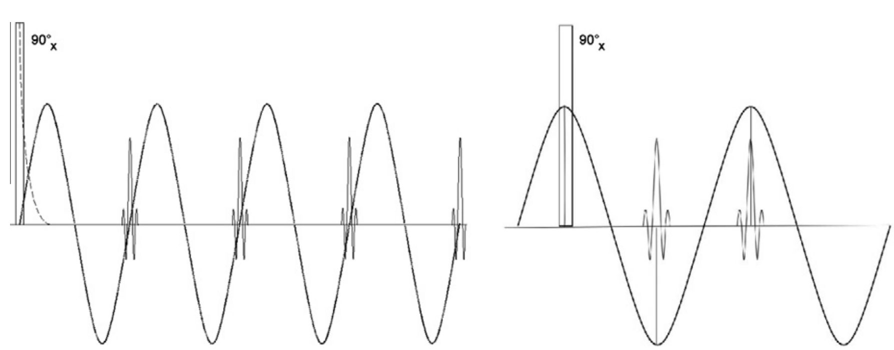

Fig. 1. *Left*: (a) schematically sketch of the ACGE-sequence. The solid curve depicts the echoes which occur after every cycle of gradient. The sampling is done at the positive-slope zero crossing of the sine-gradient (dashed curve). *Right*: (b) schematically sketch of the ACGE-sequence; the excitation is carried out during a gradient is applied, thus two echoes per cycle occur.

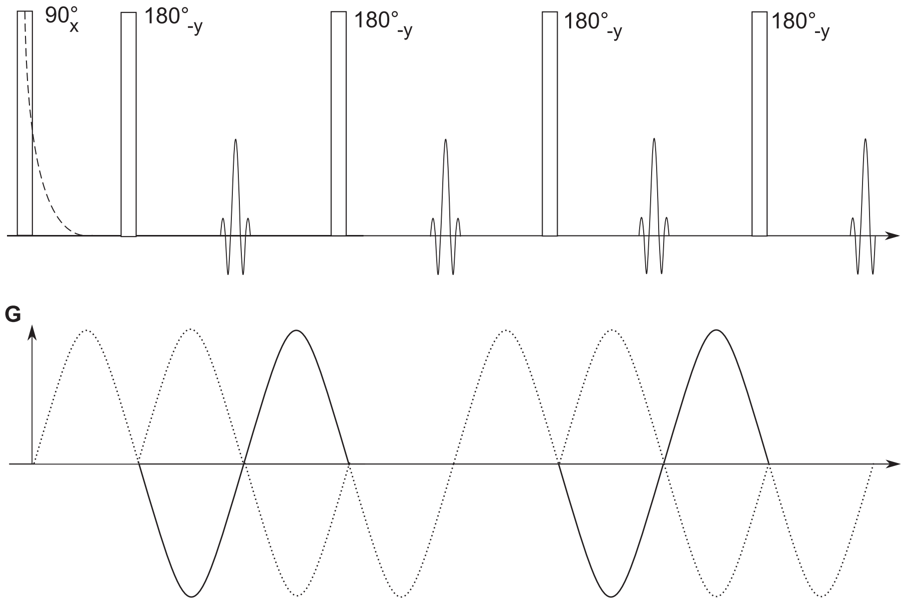

Fig. 2. Schematically sketch of the ACSE-sequence. In the lower graph the solid line is the applied sine gradient, the dotted line is the effective gradient. Note that the effective gradient integrates to zero only at even echoes; odd echoes are not expected to occur.

3. Simulations

3.1. Theoretical model

A theoretical model which is able to simulate the time-dependent signal considering the impact of plug flow as well as of a velocity distribution was developed. As an example for a velocity distribution, in this work a laminar flow velocity distribution in a cylindric volume is assumed, which implies a parabolic velocity distribution. This is a valid assumption for the parameters of the velocity and cross section of the flow phantom used in this setup. Moreover for many applications of flow measurements ideal laminar flow is a very good approximation. For velocity distributions the time-dependent signal consists of distinct parts which represent the different velocity values. On that account the velocity distribution is divided into infinitesimal velocity segments. In the case of laminar flow in a cylindrical pipe, spins of the same velocity lay on concentrical circles regarding the cross section normal to the flow direction. The spin density per velocity volume is consequently equal in all velocity segments and was therefore normalized to one. As basis for the simulation of the signal the relation for the time-dependent phase (cf. Eq. (3)) is used. Obviously only the point of acquisition is of interest. The time-dependent signal was simulated as following:

$$S(t_N) = \int_{\phi_{v_0}}^{\phi_{v_{max}}} exp(i\phi_{v'}(t_N) d\phi_{v'} \quad (6)$$

where N is the N^{th} point of acquisition. The values of the velocities where set according to the parabolic velocity distribution. Eq. (6) implicitly includes the assumption that deviation caused by spins flowing out of the sensitive area of the coil during the measurements are negligible. In the further course this will be called outflow-effect. Depending on the order of magnitude of the velocity, which is to be measured, as well as on the given parameters of the coil, considering the outflow-effect becomes essential for a correct simulation of the signal.

To simulate the outflow-effect a correction function $C(t_N)$ was introduced. $C(t_N)$ depends on the velocity v of the single segments of the velocity distribution as well as on the point of data acquisition, where t_N is the N^{th} point of acquisition. L is the length of the sensitive area of the receive coil.

$$C(t_N) = 1 - \frac{t_N v}{L} \quad (7)$$

Descriptively the correction function $C(t_N)*100$ is the percentage of excited spinvolume of the corresponding velocity segment which flew out of the sensitive volume of the coil at the time of acquisition of the N^{th} data point. The signal including the correction for the outflow-effect is simulated as following:

$$S(t_N) = S_{ideal}(t_N) * C(t_N) \quad (8)$$

Due to the outflow-effect velocity distribution of detectable excited signal is no longer parabolic. The deviation of the ideal parabolic distribution is increasing with the time of acquisition. Therefore the outflow-effect affects signal which is acquired shortly after the excitation less than data at the end of the acquisition.

3.2. Results

In order to give a short overview the signal was simulated for a stationary probe, plug flow (e.g. for the velocity of $v_{max} = 18.2$ cm/s), a parabolic flow distribution for the ideal case of an infinite sensitive area of the coil and the same parabolic distribution including the outflow-effect (see Fig. 3). The stationary spectrum (a) shows only one peak at 0 Hz with a certain spectral line width. This method does not lead to a sharp peak for a single flow velocity. The flow encoding is not constant, but constantly growing during data acquisition. This leads to a finite bandwidth as shown in Fig. 3. The spectrum of plug flow (b) is shifted by a value proportional to the velocity. The spectrum representing a parabolic velocity distribution (ideal) (c) shows a characteristic course with two distinct peaks. One is located at 0 Hz representing the stationary part of the distribution, the second peak stands for the maximum velocity of the distribution. Compared to the spectrum of plug flow the maximum peak of the distribution is shifted by the same amount. Therefore as also shown for a laminar flow, this method highlights special flow velocities like maximum or minimum flow velocity. Even though the flow velocity profile is rectangular, i.d. the number of spins with the same flow velocity is the

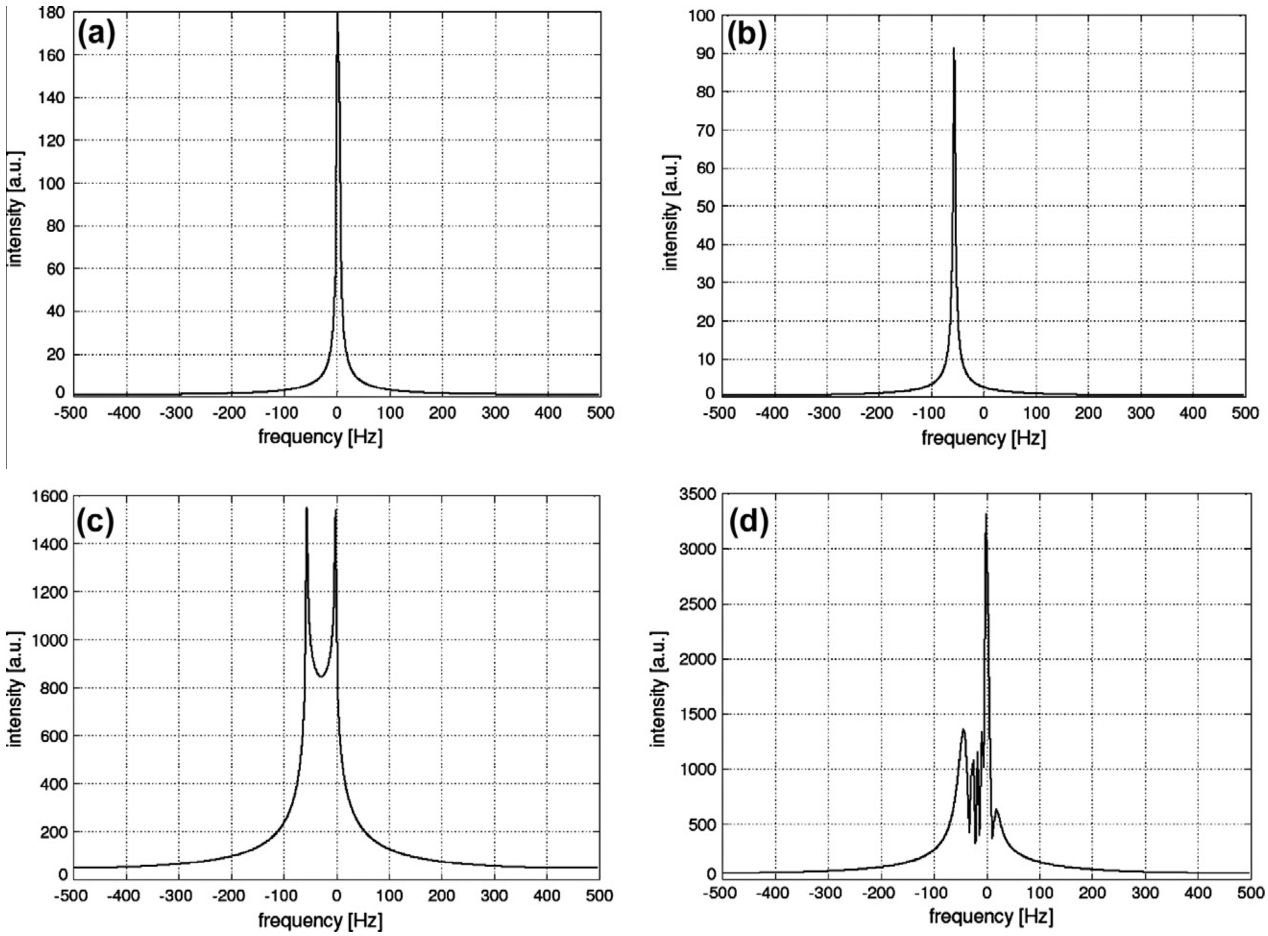

Fig. 3. Spectrum for: (a) stationary spins, (b) plug flow $v = 18.2$ cm/s with $\Delta v = -56.9$ Hz, (c) parabolic distribution with $v_{max} = 18.2$ cm/s (ideal), $\Delta v_{max} = -56.9$ Hz (d) parabolic distribution with $v_{max} = 18.2$ cm/s including the outflow-effect, $\Delta v_{max} = -45.1$ Hz.

same for all velocities in a range between maximum and zero, due to the finite linewidth for each frequency, the intensity drops to approx. 50%. However, the measured data still contain the flow profile. Spectrum (d) clearly demonstrates the influence of the outflow-effect. A significant amount of spins is leaving the receive coil during data acquisition due to increased flow. Of course this can be prevented by well adapted coil dimensions or a slice selective excitation. On the one hand the course shows a lot of small peaks on the other hand the value of the shift is smaller compared to the ideal case.

The consequences of the outflow-effect are also visible in the time-domain. The simulated signal for exemplarily values is depicted in Fig. 4, left, showing the absolute value as well as the phase in the time-domain. The absolute value of the signal shows oscillations. This can be explained by destructive interference of the single fractions of signal coming from different velocity

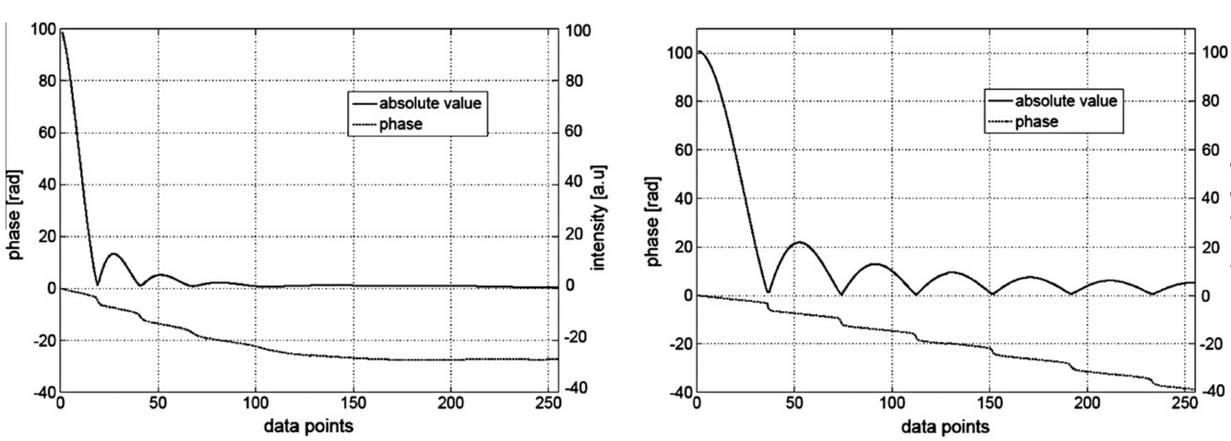

Fig. 4. *Left*: simulated signal including the outflow-effect for $\bar{v} = 9.1$ cm/s and at $G_{max} = 66$ mT/m. *Right*: simulated signal including the outflow-effect for $\bar{v} = 0.6$ cm/s and at $G_{max} = 330$ mT/m. Due to the slower velocity the outflow-effect does not have a large influence on the course of the signal. For both figures the intensity was downsized to the range of the phase.

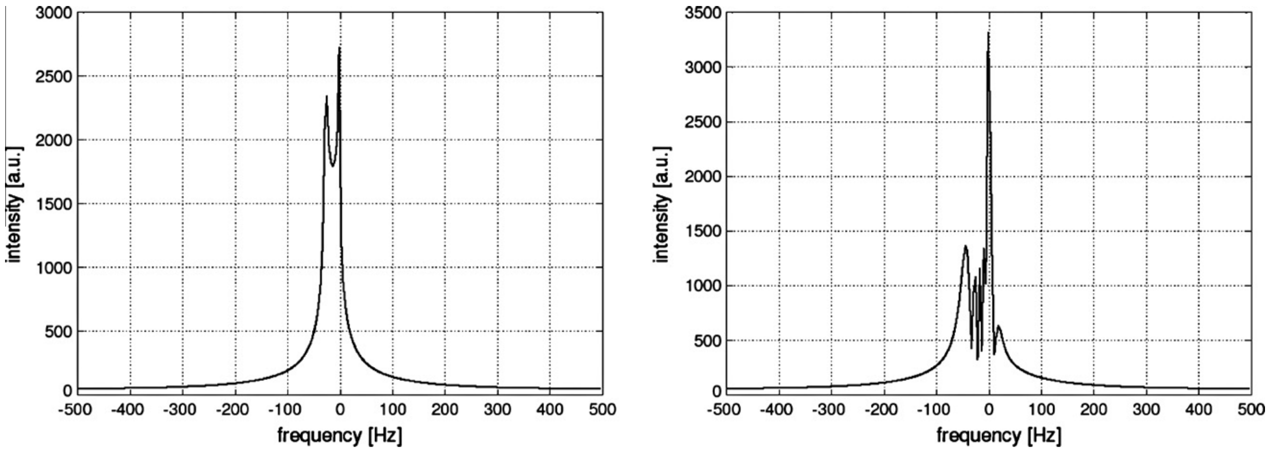

Fig. 5. *Left*: simulated spectrum including the outflow-effect for $\bar{v} = 0.6$ cm/s and at $G_{max} = 330$ mT/m. Due to the slower velocity the outflow-effect does not have a large influence on the course of the spectrum. *Right*: simulated signal including the outflow-effect for $\bar{v} = 9.1$ cm/s and at $G_{max} = 66$ mT/m. The consequence of the outflow-effect on the course of the spectrum is obvious.

segments. Owing to the outflow-effect the pattern of interference is changing in time. A signal unaffected or little affected shows a periodically interference pattern (see Fig. 4, right). At the beginning, the course of phase is linear superposed with oscillations. The oscillations of the phase are corresponding to those of the absolute value.

The Fourier Transformation converts the signal from time-domain to frequency-domain. The course of the spectra obtained is characteristic for a parabolic velocity distribution. The deviation of this ideal course of the spectrum (see Fig. 5, right) is increasing with the acquisition time as well as with increasing maximum velocity (see Fig. 5, left). For both parameters the impact of the outflow-effect is stronger for increasing parameter values.

4. Experimental results

The two pulse sequences, ACGE and ACSE were implemented on a 11.7 T *Avance 500* widebore spectrometer (Bruker Biospin GmbH, Rheinstetten, Germany). The gradient hardware had a maximum amplitude of 660 mT/m. For the measurements the maximum amplitude was limited to a value of 330 mT/m, as tests showed the gradient output was not temporally stable for values higher than the indicated one. All data were collected using a 20 mm diameter birdcage coil, the sensitive area of the coil is 40 mm in length. The flow phantom had a inner diameter of 5 mm. Laminar flow was generated by a calibrated rotary pump (*MCP-Process IP 65*, Ismatec, Zurich, Switzerland) for medium velocities of the parabolic flow distribution $\bar{v} = [0.8, 18.7]$ cm/s, for lower values $\bar{v} = [0.9, 3.9]$ mm/s a calibrated syringe pump (*Type A-99*, Fisher Scientific, Schwerte, Germany) was used.

The shape of the periodically oscillating gradient is sinus with an angular frequency of ω_G = 1 kHz or 0.5 kHz. According to the methods described above, we therefore obtain a sampling frequency of also 1 kHz or 0.5 kHz respectively. Per Scan 256 data points were collected, one measurement takes consequently 256 ms/512 ms.

4.1. ACGE – results

For test purpose ACGE scans with a stationary probe were carried out. In Fig. 6 (left) the spectrum of a stationary sample is shown. The peak is not exactly at 0 Hz and has a large line width. This is due to a nonzero dc-component of the gradient which causes a phase accumulation of stationary spins and moreover inhomogeneities. In general this is not a large effect, as state-of-the-art scanners do not show this. In this case the scanner was equipped with the original gradient coils and amplifiers from 1992.

The figure on the right shows the spectra obtained with a medium velocity of $\bar{v} = 6.18$ cm/s at a maximum amplitude of the gradient $G_{max} = 330$ mT/m. The signal could be measured for only

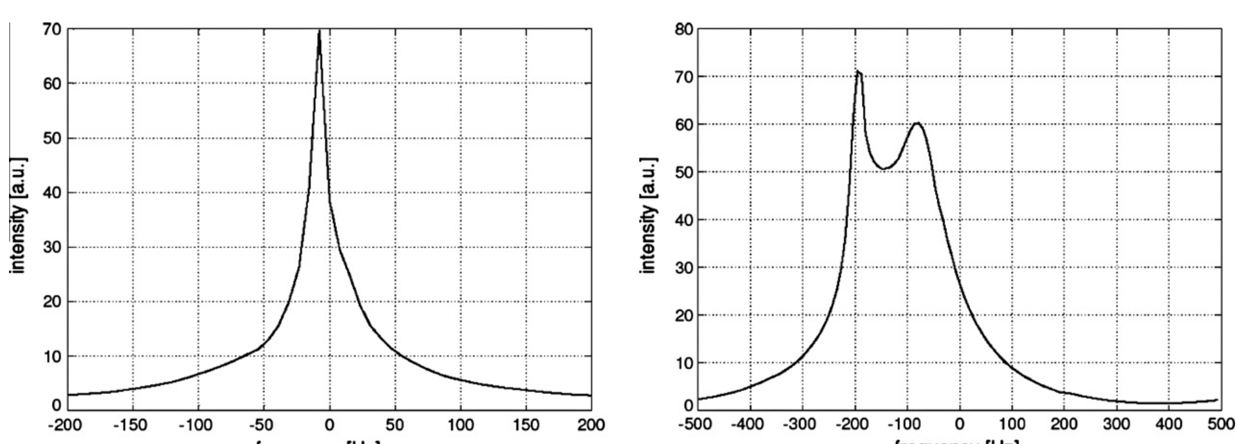

Fig. 6. *Left*: experimental spectrum for a stationary probe at $G_{max} = 66$ mT/m using the ACGE-method. *Right*: experimental spectrum for $\bar{v} = 6.18$ cm/ss at $G_{max} = 330$ mT/m using the ACGE-method.

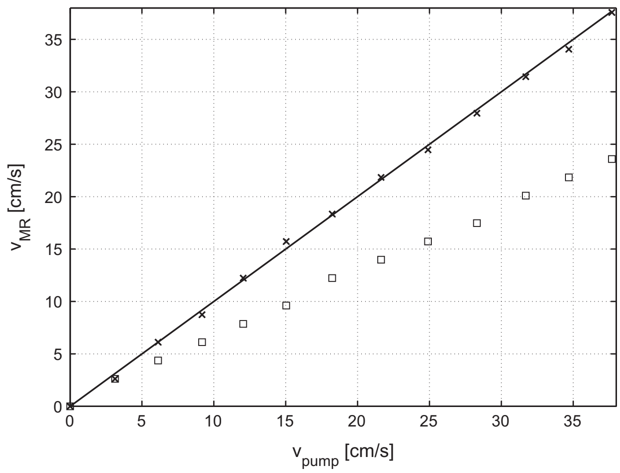

Fig. 7. Relationship between the measured maximum velocity by the shift of the spectrum and the velocity obtained by measuring the volumetric flow rate. Due to the outflow-effect with conventional evaluation v_{MR} is always smaller than the expected maximum velocity (squares). Evaluation in due consideration of the outflow-effect yields conform values for v_{MR} and v_{pump} (crosses).

~50 ms due to the fast decay of the signal as a consequence of the inaccuracies of the gradient. The course of the spectrum shows a maximum shift of $\Delta v_{max} = -191.4$ Hz, which represents the maximum velocity v_{max} of the parabolic velocity distribution. Under ideal conditions the peak at the right (at $\Delta v = -78.1$ Hz) would be at the center of the spectrum. Due to gradient inaccuracies also stationary spins acquire an additional phase. The resulting spectrum can be interpreted as a superposition of stationary and flowing spins. Phase interferences of the probe volume with different velocities can cause a resulting course as depicted in Fig. 6.

In Fig. 7 on the abscissa the maximum velocity which were adjusted on the pump are entered, on the ordinate the velocity values obtained by the measurements are plotted. The scans were carried out at a gradient strength of $G_{max} = 66$ mT/m for all scans. The solid line depicts the ideal case that the experimental results perfectly match the velocity of the pump. For the evaluation of the spectra in the first instance the maximum velocity of the distribution is calculated from the maximum shift according to Eq. (5) (squares). In the further course this will be referred to as conventional evaluation method. The deviation of the ideal case is due to the outflow-effect. It does not only have influence on the course of the spectrum but also on the size of the maximum shift. If a significant part of the spin with high velocity pass the coil during the data acquisition, as already explained above, signal from these spins cannot be detected. Consequently these spins are not represented in the frequency distribution obtained. Analyzing the data this way and not taking into account the outflow effect the measured shift is misinterpreted as the maximum velocity of a velocity distribution with a smaller maximum velocity. Knowing the coil parameters and the size of the measured shift it is possible to recalculate the actual velocity distribution. The principle is the same as done simulating the outflow-effect, just that the steps are applied reverse. For typical flow profiles like laminar flow it is possible to use a calibration curve shown in Fig. 10 (squares) or to use a previously calculated look-up table. In detail the signal was simulated including the outflow-effect as well as for ideal conditions. The velocity parameters used for simulations were the velocity ranges of the calibrated pumps. With these simulations one obtains a relation how the size of the shift with outflow-effect is correlated to the shift under ideal conditions. Therefore evaluating an experimental spectrum affected by outflow the actual shift can be determined using this relation. Based on this shift, the actual velocity can be calculated. The results are depicted in Fig. 7 (cross). It demonstrates that using the developed theoretical model and the parameters of the coil for the evaluation it is possible to determine the correct maximum velocity. This is especially an advantage over the conventional evaluation, because it can also be used for spectra strongly affected by outflow.

4.2. ACSE – results

In Fig. 8 (left) the absolute value and the phase of the signal obtained of a scan with a stationary probe is depicted. After initial oscillations caused by the even/odd-effect (further explanation below) up to the fifth data point, the phase in the time-domain shows the expected course. The inaccuracy of the gradient hardware mentioned above is compensated by the refocussing characteristic of the 180° pulses in the ACSE sequence.

However the absolute value of the signal shows another particularity (see Fig. 8, left). Theoretically it should only be possible to acquire the even echoes due to given gradients. The amplitude of the odd echoes increases quickly after some cycles of gradient and 180° pulses. The amplitude of the even echoes decreases with oscillations. In the end both types of echoes have the same amplitude. This even/odd-effect only affects the amplitude and not the phase of the signal. By averaging the even/odd pairs an almost constant result is obtained. Thus for the evaluation both types of echoes can be used. Ergo to obtain the same number of data points as

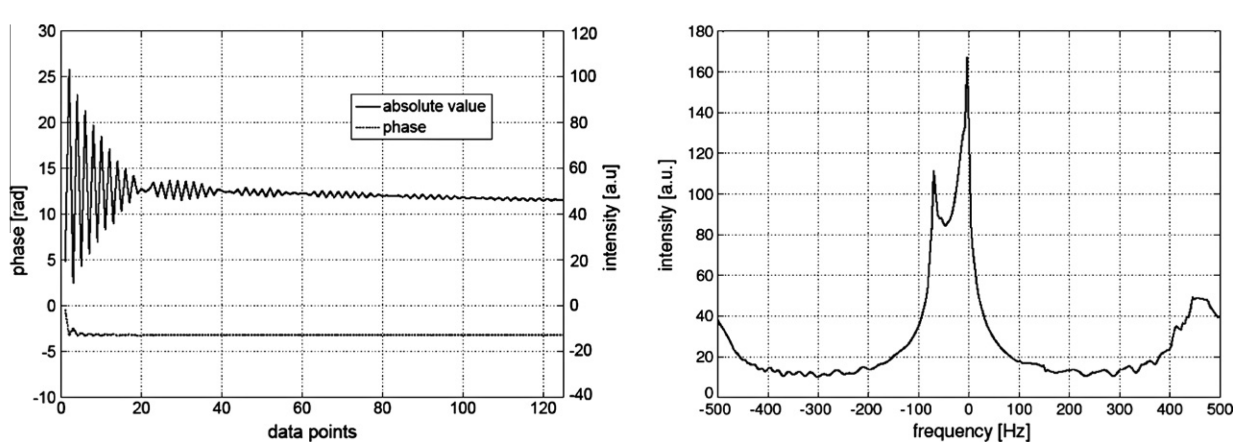

Fig. 8. *Left*: experimental data for a stationary probe at $G_{max} = 66$ mT/m using the ACSE-method (time domain). *Right*: experimental spectrum for $\bar{v} = 6.18$ cm/s at $G_{max} = 66$ mT/m using the ACSE-method.

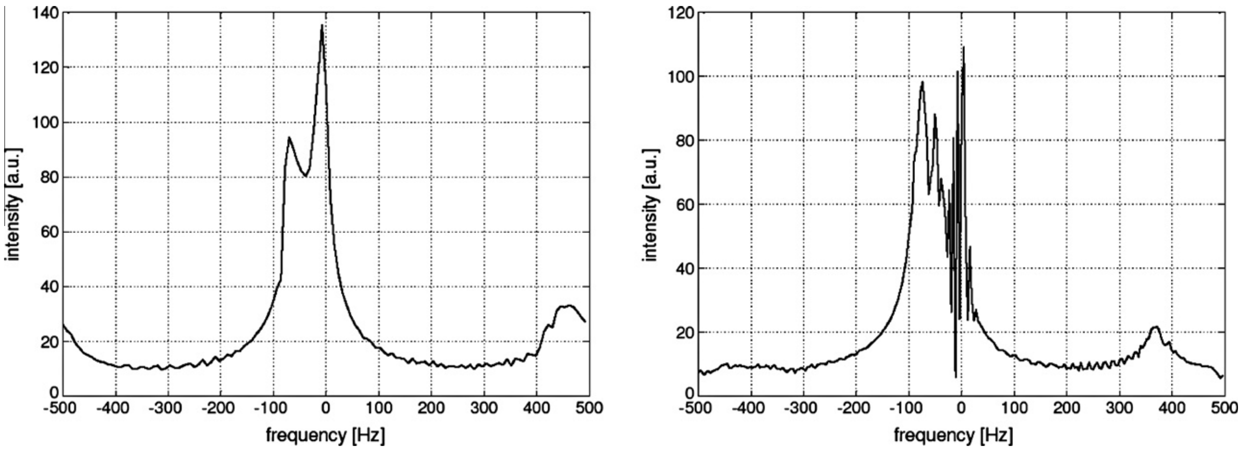

Fig. 9. *Left*: experimental spectrum for $\bar{v} = 2.9$ cm/s at $G_{max} = 132$ mT/m using the ACSE-method, $N \approx 50$ data points were acquired. *Right*: experimental spectrum for $\bar{v} = 2.9$ cm/s at $G_{max} = 132$ mT/m using the ACSE-method, $N \approx 150$ data points could be acquired.

in the ACGE sequence one does not need a longer acquisition time. The explanation for the even/odd-effect is found in the imperfections of the 180° pulses. It is likely that in reality the excitation angle is not homogenous over the whole sample. Deviating flip angles implicate an incomplete refocusing of a part of the spins. This part of the spins behaves just like the spins applying the ACGE-method. The principle of effective gradients does not hold true for these spins as the effect of gradient is not influenced by the pulse. At a pulse rate of 1 kHz, the imperfections accumulate very rapidly, so that the even/odd-effect occurs in the signal intensity. Furthermore, the pulse is not infinitely short, but has a temporal extension of 90 ms. The pulse will be applied partly under a negative, partly under a positive gradient. The stronger the gradient, the greater is the slope at the zero crossing of the sine-gradients. The area of the gradients during the pulse application increases with a steeper slope of the gradient. It turns out that at a higher gradient strength the intensities of the even and odd echoes turn into the same value more quickly.

Flow measurements at a medium velocity of $\bar{v} = 6.18$ cm/s and at a maximum amplitude of the gradient $G_{max} = 66$ mT/m with the ACSE were performed (see Fig. 8, right). The signal could be measured for ~50 ms. The spectrum shows a maximum shift of $\Delta v_{max} = -70.31$ Hz, the second is located at $\Delta v_{max} = -3.9$ Hz. This is further evidence that due to the 180° pulse train, inaccuracies are almost totally compensated, so that stationary spins of the parabolic velocity distribution do not accumulate a velocity dependent phase.

The spectra presented as yet do not show an influence of the outflow-effect. As the number of data points acquired is very small, this is consistent with the results of the simulations. To illustrate the outflow-effect on the course of the spectrum, the following figure (see Fig. 9) shows two scans with exactly the same parameters besides the time of acquisition and accordingly the number of points acquired. For $N \approx 50$ the spectrum shows the known course. The spectrum obtained with $N \approx 150$ holds not only two maxima, but several smaller peaks, especially around the center of the spectrum. However also in this spectrum a distinct maximum peak of the same shift is observable. The course of the spectrum is explicable by the outflow-effect. The percentage of the whole signal, which is affected significantly by the outflow-effect is high for the chosen parameters of velocity and sensitive area of the coil. On the one hand the spectrum is a superposition of the signal acquired at the beginning and consequently representing a parabolic velocity distribution. On the other hand a fraction of the signal represents a velocity distribution resulting from the limited measuring range. The superposition of these two components yields the depicted course. Despite the very different courses the value of the frequency shift is the same, e.g. they obtain the same information. Therefore to determine the shift it is not essential to acquire a lot of data points. The main advantage of increasing the number of data points is that the resolution of the spectra is increasing with the number of points. The error of the shift due to the limiting factor of resolution is consequently less.

Also for this method quantitative flow measurements at a constant maximum gradient of $G_{max} = 66$ mT/m were carried out (see Fig. 11). The evaluation was done conventionally (squares) and in due consideration of the outflow-effect (crosses). Similar to the ACGE results also in this case the conventional evaluation yields to systematically underestimated flow velocities, whereas the results obtained in due consideration of the outflow-effect match with the velocities adjusted on the calibrated pump.

As the obtained shift with the same parameters is twice as large as for the ACGE – method, the following figure shows the obtained results for a velocity range of [mm/s]. As the distance of the spins moving during acquisition is, compared to the length of the coil,

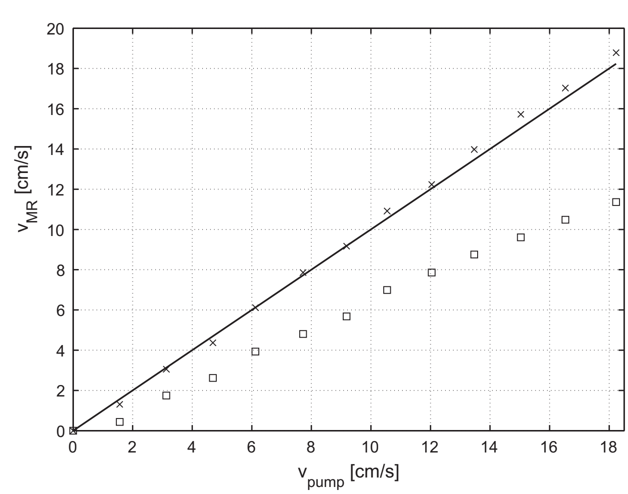

Fig. 10. Relationship between the measured maximum velocity by the shift of the spectrum and the velocity obtained by measuring the volumetric flow rate. Due to the outflow-effect with conventional evaluation v_{MR} is always smaller than the expected maximum velocity (squares). Evaluation in due consideration of the outflow-effect yields conform values for v_{MR} and v_{pump}.

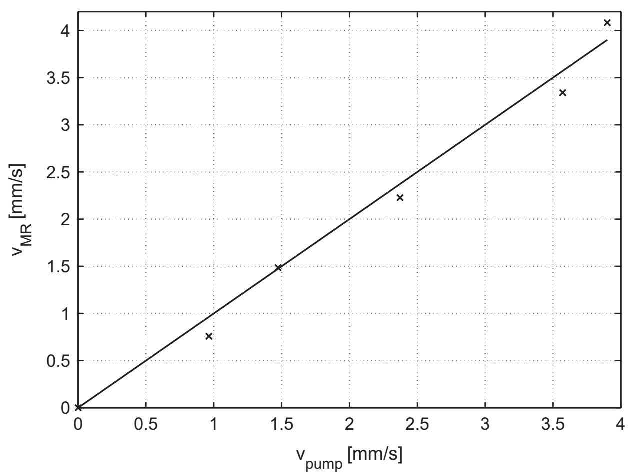

Fig. 11. Relationship between the measured maximum velocity by the shift of the spectrum and the velocity obtained by measuring the volumetric flow rate. The data was obtained using a gradient of $G_{max} = 330$ mT/m.

relatively small there was no need for a correction of the outflow-effect.

5. Discussion

In the preceding sections a spectroscopic method to quantitatively measure velocities with MR has been introduced. This work has sought to firstly develop a theoretical model which describes the characteristics of this method by means of parabolic velocity distributions and additionally the theoretical model combined with the description of the outflow-effect. The simulations allow a correct prediction of the value of the maximum shift and furthermore they also show the right course of the spectrum and the time-domain signal. This has been essential for understanding the effects of the parabolic velocity distribution and of the time-dependent outflow-effect. The ACGE and ACSE were implemented on a 11.7 T *Avance 500* spectrometer. The requirements for the hardware are low as the waveshape of the gradient only has to be periodic with zero average component. Moreover it does not need to be sinusoidal or even symmetric.

With both pulse sequences presented above it was demonstrated that they can perform quantitative velocity measurements. Depending on the chosen parameters of gradient strength and angular frequency of the gradient, which is corresponding to the sampling rate, it is possible to measure velocities distributions within the range of mm/s (with ACSE) up to cm/s (with ACSE and ACGE). Using the theoretical model for evaluating the experimental spectra it is possible to correctly evaluate the spectra even if they are strongly affected by outflow, so that the conventional way of evaluation would give wrong results with underestimated maximum velocity. The length of the sensitive area of the coil is therefore not a limiting factor for most of the parameter combinations of L and v_{max}. The ACGE as well as the ACSE method are fast, single-shot techniques, which convert velocity to frequency shift. For the ACGE the signal is decaying with T_2^* and it requires a sufficient field homogeneity. Given a set-up providing this characteristic, the ACGE – method is the simplest implementation of a spectroscopic measurement. In contrary to ACGE the ACSE has very low demands on field homogeneity due to the 180° pulse train. By compensating field inhomogeneity the signal is longer detectable as it only decays with T_2. Furthermore the obtained value of shift is twice as large with ACSE at constant parameters. As for both sequences the resolution of the spectrum is the lower limit of measurable velocities, with ACSE smaller velocities are detectable. In fact, the high number of refocusing pulses given in a short time period, compared with other methods, increases the specific absorption rate (SAR) which may be crucial at high field. Generally speaking the ACSE offers a larger area of application as the advantages are prevailing. Outflow is a general problem in flow measurements. Similar to standard flow measurements the signal is unaffected by spins, that have already left the receive coil during signal reception. In general this results in signal loss and flow velocity underestimation, since especially all fast spins have left the coil. Typically this deviation is averaged to a single phase value, leading to a systematic error similar to the one shown in Fig. 7 if no correction is applied. The behavior is different for the shown method which leads to spectra depicting multiple peaks. Referring to the course of the spectrum, the peak representing the maximum measurable velocity is unaffected by this behavior. This means the peak is still unambiguously identifiable. But nevertheless for a quantitative evaluation of the spectra one has to keep in mind that this peak only represents the maximum velocity of spins that have not left the coil during data acquisition (like any other method as well). In comparison to this work Walton et al. basically showed that due to flowing spins a shift is detectable, but no further quantification of the measured velocity or velocity distribution were carried out. Furthermore the interpretation of the course of the spectra and consequently a quantifying evaluation was not performed. Moreover the outflow-effect was not considered, which is essential to obtain the correct velocity value especially for velocities in the range of [cm/s] as they were also used by Walton et al.

Additionally the acquisition of both pulse sequences, which was so far singlepoint acquisition, was modified so that not only one point per echo was acquired. Each echo was covered by 128 data points, which were symmetrically sampled to the middle of the echo. As the phase of the signal is constant around the center of the echo, these points are used for averaging. For this special set-up $N \approx 10$ points per echo seem to be beneficially combinable. By averaging the SNR is increased by $\sqrt{N}$ without additional time of acquisition.

Both methods appear useful for the application of quantitative, rapid velocity measurements where no localization is needed. Especially for probes with a large stationary volume velocity can easily be detected as the spectrum will show a distinct peak for the maximum velocity and stationary spins are totally unaffected by the pulse sequences. If the outflow-effect is insignificant, the spectrum shows a characteristic course with two distinct peaks for parabolic distributions. From this spectrum a quantitative determination of the maximum velocity is possible. For the case of parabolic velocity distributions the results proofed that a correct evaluation of spectra strongly influenced by outflow is feasible. Though the frequency shift is directly proportional to the velocity, this technique is not suitable for a quantification of the single velocity-components of a velocity distributions in general. As it was shown in this work, a theoretical model is essential for the correct evaluation and interpretation of the experimental data. The presented methods are not limited to pure spectroscopic measurements. The issue of combing these methods with a spatial localization needs to be addressed in future work.

References

[1] A. Caprihan, J.G. Davis, S.A. Altobelli, E. Fukushima, A new method for flow velocity measurement: frequency encoded NMR, Magn. Reson. Med. 3 (2) (1986) 352–362.

[2] C. Dumloulin, S. Souza, C.J. Hardy, S.A. Ash, Quantitative measurement of blood flow using cylindrically localized fourier velocity encoding, Magn. Reson. Med. 21 (1991) 242–250.

[3] D.J. Bryant, J.A. Payne, D.N. Firmin, D.B. Longmore, Measurement of flow with NMR imaging using a gradient pulse and phase difference technique, J. Comput. Assist. Tomogr. 8 (4) (1984) 588–593.
[4] E. Fukushima, Nuclear magnetic resonance as a tool to study flow, Annu. Rev. Fluid Mech. 31 (1999) 95–123.
[5] G.B. Pike, C.H. Meyer, T.J. Brosnan, N.J. Pelc, Magnetic resonance velocity imaging using a fast spiral phase contrast sequence, Magn. Reson. Med. 32 (4) (1994) 476–483.
[6] E.L. Hahn, Detection of sea-water motion by nuclear precession, J. Geophys. Res. 65 (1960) 776–777.
[7] J.H. Walton, M.S. Conradi, Flow velocity measurement with ac gradients, Magn. Reson. Med. 4 (1987) 274–281.
[8] P.R. Moran, A flow velocity zeugmatographic interlace for NMR imaging in humans, Magn. Reson. Imag. 1 (1982) 197–203.
[9] E. Stejskal, Use of spin echoes in a pulsed magnetic-field gradient to study anisotropic, restricted diffusion and flow, J. Chem. Phys. 43 (1965) 3597–3603.
[10] J. Suryan, Nuclear resonance in flowing liquids, Proc. Indian Acad. Sci. Sect. A 33 (1951) 107–111.